Translational Science

Cancer Research

# Age-Dependent Cellular and Behavioral Deficits Induced by Molecularly Targeted Drugs Are Reversible

Joseph Scafidi[1,2], Jonathan Ritter[2], Brooke M. Talbot[2], Jorge Edwards[2], Li-Jin Chew[2], and Vittorio Gallo[2]

## Abstract

Newly developed targeted anticancer drugs inhibit signaling pathways commonly altered in adult and pediatric cancers. However, as these pathways are also essential for normal brain development, concerns have emerged of neurologic sequelae resulting specifically from their application in pediatric cancers. The neural substrates and age dependency of these drug-induced effects *in vivo* are unknown, and their long-term behavioral consequences have not been characterized. This study defines the age-dependent cellular and behavioral effects of these drugs on normally developing brains and determines their reversibility with post-drug intervention. Mice at different postnatal ages received short courses of molecularly targeted drugs in regimens analagous to clinical treatment. Analysis of rapidly developing brain structures important for sensorimotor and cognitive function showed that, while adult administration was without effect, earlier neonatal administration of targeted therapies attenuated white matter oligodendroglia and hippocampal neuronal development more profoundly than later administration, leading to long-lasting behavioral deficits. This functional impairment was reversed by rehabilitation with physical and cognitive enrichment. Our findings demonstrate age-dependent, reversible effects of these drugs on brain development, which are important considerations as treatment options expand for pediatric cancers.

**Significance:** Targeted therapeutics elicit age-dependent long-term consequences on the developing brain that can be ameliorated with environmental enrichment. *Cancer Res; 78(8); 2081–95.*




## Introduction

Primary central nervous system (CNS) tumors continue to be the leading type of solid tumors in the pediatric oncology population (1, 2). Treatment strategies using a combination of cytotoxic chemotherapy, radiation, and surgery have greatly improved patient survival. However, the rapidly developing brains of children are particularly susceptible to long-term neurologic sequelae from brain tumors and their treatment, thus contributing to an increased incidence of morbidity (3). Therefore, it is necessary to develop newer treatment paradigms that target proliferating cancer cells, while sparing the cytotoxic effects of conventional chemotherapeutic agents and radiotherapy on the developing brain.

There has been significant progress made in understanding the molecular pathways responsible for tumor growth. Interestingly, many of these pathways are especially active during brain development. A pathway shared by different cancers involves dysfunctional receptor tyrosine kinases (RTK) signaling. During normal brain development, RTKs are key regulators of proliferation, mitogenesis, survival, metabolism, and migration of neural progenitor cells. Overexpression, amplification, or mutation of RTKs, such as EGFR, VEGF receptor (VEGFR), and platelet-derived growth factor receptor (PDGFR), are implicated in tumorigenesis (4). Expression of these RTKs often correlates with tumor grade and a poor prognosis. They are highly expressed in high-grade gliomas, medulloblastomas, ependymomas, and diffuse intrinsic pontine gliomas, all of which are commonly found in the pediatric population (5).

The PI3K pathway is an RTK-driven downstream signaling pathway whose main target is the master regulator mTOR, a serine/threonine intracellular kinase. These PI3K/mTOR signaling pathways control neural progenitor growth and migration during brain development (6–8), and are upregulated in multiple CNS neoplasms in both pediatric and adult cancers (9).

Our understanding of cancer pathways have resulted in the development of molecularly targeted drugs. This class of drugs was developed to be cystostatic and inhibit tumorigenesis. They are ideal candidates for treating brain tumors because their low molecular weight enables them to permeate the blood–brain barrier. Drugs such as gefitinib (Iressa) and sunitinib malate (Sutent) target EGFR and VEGFR/PDGFR, respectively. These drugs are currently used in monotherapy, in combination therapy, or as radiosensitizers (7, 10–13). Rapamycin (sirolimus) is an inhibitor of the mTOR pathway, which is used for low-grade gliomas and subependymal giant cell astrocytoma's in children

[1]Neurology, Children's National Health System, Washington, D.C. [2]Center for Neuroscience Research, Children's Research Institute, Children's National Health System, Washington, D.C.

**Note:** Supplementary data for this article are available at Cancer Research Online (http://cancerres.aacrjournals.org/).

**Corresponding Author:** Joseph Scafidi, Center for Neuroscience Research, Children's National Medical Center, 111 Michigan Avenue, NW, Washington, D.C. 20010-2970. Phone: 202-476-6144; Fax: 202-476-2864; E-mail: jscafidi@childrensnational.org

**doi:** 10.1158/0008-5472.CAN-17-2254

with tuberous sclerosis (14, 15). Significant responses in certain cancer types are evident when these drugs are delivered individually or in combination with traditional approaches (16). However, most preclinical and clinical studies have been conducted in adults, in whom the targeted pathways are not as active (17). Interest in using these targeted drugs for cancer in childhood and adolescents is increasing, but the effects of these agents on normal noncancerous cells in the young developing brain are unknown (18, 19). It is imperative to understand whether these molecularly targeted drugs affect normal cellular development at a time when younger brains have larger populations of immature cells that continue to undergo significant postnatal development.

In this study, we investigated the short- and long-term cellular and behavioral effects of gefitinib, sunitinib, and rapamycin in the cerebral white matter and hippocampus, brain regions that exhibit a continuum of rapid postnatal development from infancy to late adolescence (20–24). Evidence suggests that molecularly targeted drugs may have less detrimental effects on brain function than current treatments (25, 26). Gefitinib, sunitinib, and rapamycin inhibit specific pathways commonly altered in various pediatric cancers, including brain tumors. We sought to define the broad effects of these drugs on the developing brain and to determine whether their effects are developmentally regulated. We used normal naïve mice in paradigms that mimic typical cancer therapy protocols. We compared these effects with adult treatment paradigms. Furthermore, we examined whether the sensorimotor and neurocognitive deficits of these drugs are mitigated by physical and cognitive enrichment, which is analogous to similar enrichment therapies recently found beneficial in patients undergoing cancer treatment (27, 28). Our study is the first to demonstrate age-dependent effects of molecularly targeted drugs on critical brain structures and reversal of these age-dependent deficits with nonpharmacologic interventions.

## Materials and Methods

### Drug exposure paradigms

All procedures performed on mice were approved by the Institutional Animal Care and Use Committee of Children's National Medical Center and adhered to the Guide for the Care and Use of Laboratory Animals (NIH, Bethesda, MD).

C57BL/6 wild-type mice or *GAD2-IRES-Cre*-R26R-EYFP mice (The Jackson Laboratory stock #010802 and #006148, respectively) were randomized to vehicle or one of the three molecularly targeted drugs. They were further randomized to one of two developmental paradigms: paradigm 1 or paradigm 2 (Fig. 1A–C). Mice randomized to paradigm #1 (early development, ED) received either vehicle or drug from postnatal day 12 (P12) to P17. Mice randomized to paradigm #2 (late development, LD) received either vehicle or drug from P17 to P22. In a separate set of experiments, adult male and female mice between 12 and 14 weeks of life (adulthood) were randomized to receive daily doses of vehicle or drug for 6 days (adult paradigm). Vehicle or drugs were administered systemically via intraperitoneal injection at the same approximate time each day to reduce the risk of toxicity. Mice in all paradigms received an equal number of drug or vehicle doses.

Vehicle- and drug-containing solutions were a 75% to 25% ratio of sunflower seed oil (Sigma Aldrich) and dimethyl sulfoxide (DMSO; Sigma-Aldrich), in which DMSO was used as a solubilizing agent. Molecularly targeted agents used for this study included: (i) gefitinib (Tocris), a selective EGFR antagonist, administrated at 70 μg/g/day (29); (ii) sunitinib malate (Tocris), a multiple receptor tyrosine kinase (RTK) inhibitor acting mainly on the platelet-derived growth factor (PDGF) beta (β) and VEGF receptors, administrated at 35 μg/g/day (30, 31); and (iii) rapamycin/sirolimus (Tocris), a potent mTOR inhibitor, administered at 1 μg/g/day (32).

We confirmed the expression profile of these drugs' targets in the white matter and hippocampus (Supplementary Fig. S1A). We also confirmed that these doses of medication chosen from the literature did not cause mortality and that they inhibited their specific targets in the brain (Supplementary Fig. S1B).

### BrdUrd pulse protocol

The 5-bromo-2′-deoxyuridine (BrdUrd) pulse protocol used in these studies has been described previously (31). Briefly, mice were administered BrdUrd (Sigma) over a period of four days, according to the paradigm. The injections were administered

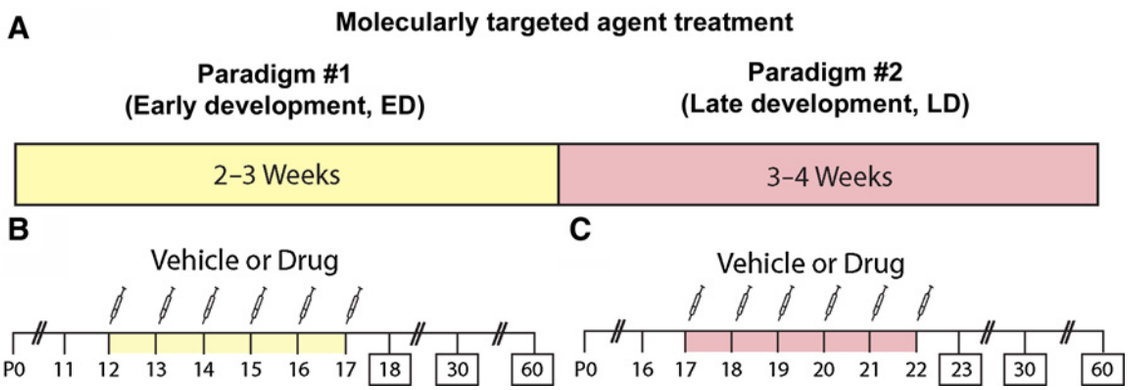


**Figure 1.**

Molecularly targeted agent treatment paradigms at different developmental stages. **A,** Visual representation of the two paradigms. Paradigm #1 represents early development (ED), corresponding to approximately the second to third week of life in the mouse. Paradigm #2 represents later development (LD), corresponding to approximately 3–4 weeks in the mouse. **B** and **C,** The timeline for each paradigm and the sacrifice points. Behavioral testing was performed at 1 month and 2 months of age in naïve groups of mice. Days of drug exposure are denoted with a syringe over the postnatal day.

intraperitoneally at approximately the same time each day and 8 hours prior to vehicle or drug administration to prevent toxicity.

### IHC

Mice were anesthetized with isoflurane and transcardially perfused with 0.1 mol/L PBS, followed by 4% paraformaldehyde (PFA) overnight at 4°C. Brains were then transferred to 20% glycerol (w/v) followed by 10% glycerol. Serial coronal sections (35–40 μm thick) were cut using a sliding microtome with freezing stage (Thermo Fisher Scientific) and stored in a 0.05% sodium azide/PBS solution. IHC was performed on free-floating sections by first placing slices in blocking solution [1% BSA, 0.3% Triton X-100, and 20% normal goat serum (NGS) in 1× PBS] for 1 hour at room temperature. Tissue analyzed for BrdUrd incorporation was pretreated prior to blocking solution with 2 N HCl for 30 minutes, followed by 0.1 mol/L boric acid for 15 minutes at room temperature.

All primary and secondary antibodies were diluted in carrier solution [1% BSA, 0.3% Triton X-100, and 1% NGS in 1× PBS]. Sections used for IHC were incubated in primary antibodies at 4°C overnight. The following primary antibodies and concentrations were used: mouse CC1, rabbit Olig2, rabbit NG2 chondroitin sulfate proteoglycan, rabbit cleaved (activated) caspase-3 (Casp-3), and guinea pig doublecortin (DCx) antibody were diluted 1:500 (EMD Millipore); chicken antibody glial fibrillary acidic protein (GFAP) was diluted 1:1,000 (Abcam); mouse glutamine synthetase (GS), rabbit Sox2, chicken GFP and rabbit BrdUrd antibody were diluted 1:500 (Abcam); mouse NeuN antibody was diluted 1:250 (EMD Millipore); and rabbit Ki67 antibody was diluted 1:500 (Vector Laboratories). Slices were rinsed with 1× PBS three times and placed in carrier solution containing secondary antibodies. The following secondary antibodies at a concentration of 1:200 were used (Jackson Immunoresearch Laboratories): FITC-conjugated goat anti-mouse IgG; FITC-conjugated goat anti-rabbit IgG; FITC-conjugated goat anti-chicken IgG; CY5-conjugated goat anti-mouse IgG; CY5-conjugated goat anti-rabbit IgG; CY3/rhodamine-conjugated goat anti-mouse IgG; and CY3/rhodamine–conjugated goat anti-rabbit IgG. Sections were incubated with secondary antibodies for 1 hour at room temperature, followed by a 10-minute incubation with DAPI (1:500; Invitrogen, D1306), washed with 1× PBS three times, and mounted using mowiol.

### Confocal microscopy and quantitative analysis

IHC imaging was conducted with a Zeiss confocal laser scanning microscopic described previously (33). Optical sections were acquired with the use of ZEN software, under a 40× objective. Four different laser lines were used for imaging: FITC (488 nm excitation; 522/35 emission filter); Cy3 (560 nm excitation; 605/32 emission filter); Cy5 (647 nm excitation; 680/32 emission filter); and DAPI (400 nm excitation). The images were acquired with a z step size of 1μm. The z-stack was viewed using NIH ImageJ and Zeiss LSM Image Browser (version 4.2). Immunolabeled cells were manually counted in each optical section using the ImageJ "Cell Counter" plugin. An average of 6 images were taken for each section (3 tissue sections for each animal) from the white matter, including 2 from the corpus callosum, two from the cingulum, and 2 from the external capsule regions. An average of 12 images was taken for each section (3 tissue sections for each animal) from the CA1, CA3, and DG regions of the hippocampus. Images used for publication were created using ImageJ and Photoshop (CS5) software.

### Western blotting

Protein quantification analysis was conducted on microdissected white matter and hippocampal tissue. The white matter tissue included the corpus callosum, cingulum, and external capsule. Hippocampus tissue included both sides of the entire hippocampus. Samples were homogenized in RIPA lysis buffer with proteinase inhibitors (Millipore 20-188). Proteins were quantified using the Pierce BCA kit (Thermo Fisher Scientific). For gel electrophoresis, equal amounts of protein (10–20 μg) were loaded for each sample on 4%–20% pre-cast Tris-glycine gradient gels. The gels were transferred onto polyvinylidene difluoride membranes using the Trans-Blot Turbo Transfer System (Bio-Rad). Immunoblotting was performed by first blocking membranes in 3% BSA in Tris-buffered saline with 1% Tween-20 (TBST) for 1 hour at room temperature. Membranes were then incubated overnight at 4°C in a primary antibody solution of 3% BSA in TBST. The following concentrations were used for primary antibodies: mouse β-actin-horseradish peroxidase (HRP) antibody diluted at 1:5,000 (Abcam); rabbit phosphorylated (p) EGFR diluted at 1:1,000 (Novus Biologicals); rabbit pPDGFRβ diluted at 1:1,000 (Abcam); rabbit pVEGFR diluted at 1:1,000 (Millipore); rabbit pmTOR diluted at 1:1,000 (Cell Signaling Technology); mouse myelin basic protein (MBP) antibody diluted at 1:1,000 (Covance); and chicken glial fibrillary acidic protein (GFAP) antibody diluted 1:1,000 (Abcam). Membranes were then washed three times in TBST and incubated with each respective HRP-conjugated antibody in 3% BSA in TBST. The following secondary HRP-conjugated antibodies were used: goat anti-rabbit and anti-mouse (Santa Cruz Biotechnology), and goat anti-chicken (Aves Labs Inc.) were diluted 1:5,000 in 3% BSA in TBST. Chemiluminescent detection was performed using ECL Super-Signal (Thermo Fisher Scientific) kits according to manufacturer's directions. A pair-wise comparison between vehicle and drug treatment groups for all study time points was performed for analysis of Western blots. For all samples, the optical density for each protein of interest was determined and expressed as a ratio of the internal control β-actin.

### Behavioral assessment

All behavioral tasks to assess both white matter and hippocampal function were performed on C57BL/6 wild-type mice that had not undergone any previous behavioral testing and had been accustomed to being handled by the investigators. The investigator that performed behavioral testing was blinded to treatment group and paradigm, but not sex or age. Males and females were used for these studies with no mice or results excluded from behavioral testing. Mice were acclimated to the behavioral testing room for one hour prior to commencement of testing. Mice were kept on a regular 12-hour light/dark cycle (6 am–6 pm), with food and water made available *ad libitum*. All behavioral experiments were performed in the evening, when mice are most active. The order of testing for each mouse was as follows: inclined beam-walking task; novel object recognition; spontaneous alternation behavioral testing on Y-Maze for P30. Mice tested at P60 underwent same testing order; however, the spontaneous alternations Y-maze behavior test was substituted with the Barnes Maze. All behavioral testing was performed in the same suite under the same lighting conditions except for the Barnes Maze, which required the addition of a bright overhead lamp with light directed at the center of the maze.

***Inclined beam walk.*** The inclined-beam test is used to assess sensory–motor integration and the overall function of the subcortical WM, as described previously (33). Mice were subjected to behavioral assessment at P30 and P60. The task involved two separate beams (2 and 1 cm), each inclined at 30 degrees, with a target box placed at the top of beams for the mice to reach. The beam was cleaned with 30% ethanol (v/v) between each mouse. The number of front and hind leg foot slips off of the beam was quantified for each mouse as the mice traversed the length of each beam.

***Novel object recognition.*** This hippocampal-dependent test assesses recognition memory (34). Mice were habituated to an opaque rectangular field measuring 27 × 27 × 20 cm for 5 minutes on the day prior to and during the day of testing. The open field was cleaned with 30% ethanol (v/v) between each mouse to minimize olfactory cues. In the familiarization phase, two identical objects were placed equidistant and 5 cm away from the walls of the open field. The mouse was placed in the open field with its head facing the experimenter and opposite to the objects. The experiment was stopped when 30 seconds of exploration between both objects was reached, or when a 5-minute period had passed. The mouse was then returned to the home cage and the open field and objects were cleaned with 30% ethanol (v/v). The test session was performed 12 hours later. One of the objects was replaced with a novel object, and the familiar object was replaced to ensure no residual olfactory cues on the previously used object. The mouse was placed in the field facing the experimenter and the time to explore each object was recorded. The experiment stopped when the mouse had explored both objects for a total of 30 seconds. The mouse was returned to the home cage and the objects and open field were cleaned with 30% ethanol (v/v) to minimize olfactory cues between mice. The time it took (seconds) to reach the criterion of 30 seconds and the amount of time spent with each individual object was recorded. Data presented are the amount of time spent with the novel object over the total exploration time (30 seconds). This percentage/ratio was then used for statistical analysis.

***Continuous spontaneous alternations Y-Maze behavior.*** As described in ref. 35, mice were placed in the center of a Y-maze and allowed 8 minutes to freely explore the open three arms of the Y-Maze labeled A, B, or C. Activity was recorded with a video camera centered above the maze. Each arm choice was recorded during this 8-minute period. The mouse was returned to the home cage and the Y-Maze is cleaned with 30% ethanol (v/v) between mice. The spontaneous alternation behavior is scored by determining the number of three unique arm entries (alternation) divided by the total number of arm entries minus 1 (35). The spontaneous alternation Y-Maze behavior testing was performed only on P30 mice.

***Barnes maze.*** The Barnes maze is a dry land-maze test for hippocampal dependent spatial learning and memory. The Barnes maze is like the Morris Water Maze and radial arm maze, but does not require strong aversive stimuli or deprivation. The circular platform (92 cm in diameter) has 20 equally spaced open holes (5 cm in diameter and 7.5 cm between holes) along the perimeter. Mice were trained to use spatial cues around the room to locate the hole directly over a darkened escape box. ANY-maze (Stoelting Co.) tracking software with video camera was used. The mice were habituated on day 1 by placing them in the center of the maze covered by a dark cylinder for 15 seconds. A bright light above the platform shines directly on the platform. The mouse was gently guided to the escape hole and allowed to remain in the escape box for 2 minutes. Then the mouse was returned to the home cage. The maze was cleaned with 30% ethanol (v/v) and rotated while maintaining a constant location of the escape hole. During the training phase on days 1–5, three trials with an inter-trial interval of 15 minutes were performed. Mice were placed in the center of the platform covered by a dark cylinder for 15 seconds. The trial ended when the mouse enters the escape hole or 3 minutes have elapsed. If the mouse was unable to locate the escape box, the mouse was gently guided there and allowed to remain inside for 1 minute. Short-term memory was tested, 24 hours after last training day (probe day 1), by determining the mouse's memory of the target hole location within 90 seconds. All holes were blocked and the mouse was unable to escape. Long-term memory was assessed with a test day 5 days after the first Probe day (probe day 5). The number of errors and latency until the escape hole was located (primary errors and primary latency, respectively) was determined. The Barnes Maze was performed at P60 because of inability to reliably train mice in the drug treatment groups at P30.

***Environmental enrichment.*** Naïve C57BL/6 wild-type male and female mice were randomized to either receive vehicle or one of the three drugs. Only Paradigm #1 (ED) was utilized for this study. The mice were further randomized to typical housing or in an enriched environment beginning on P17. As described previously, the enriched environment consisted of 6–8 mice per cage with a dimension of 29 × 18 × 12.5 cm ($L \times W \times H$; ref. 36). The enriched cages were equipped with a running wheel, a set of plastic tubes of different textures and sizes, and various toys. Objects in the enriched cages were changed every 3 days and rearranged to maintain novelty. Mice were housed in the enriched cages only during the dark cycle. They were returned to their home cage during the light cycle. Food and water was available *ad libitum*.

### Statistical analysis

The data contained in all histograms and line graphs are presented as averages ± the SEM and created using GraphPad Prism 7.0. All cell quantification and Western blot data were compared using one-way ANOVA analysis to determine whether an overall statistically significant difference existed between study groups at specific ages. Each respective drug group was compared against the vehicle study group and adjusted using Bonferroni correction. The Bonferroni correction was applied for the following comparisons: vehicle versus gefitinib, vehicle versus sunitinib, and vehicle versus rapamycin. A two-tailed type I error ($P < 0.05$) was used to determine statistical significance. The degree of statistical significance was denoted using asterisks ($^{*}$, $P < 0.05$; $^{**}$, $P < 0.01$; $^{***}$, $P < 0.005$). The data from foot slips (inclined beam walk), novel object recognition (NOR), spontaneous alternation behavior (Y-maze), and Barnes maze were also analyzed using one-way ANOVA. The same Bonferroni correction was applied for the comparisons listed above. Regarding the studies on environmental enrichment, a one-way ANOVA was performed on all groups to determine whether an overall statistically significant difference existed. Each respective enriched group was compared against the nonenriched group and adjusted using an unpaired *t* test. A two-tailed type I error ($P < 0.05$) was used to determine statistical significance.

### Data availability

All relevant data are available from the authors.

## Results

### Molecularly targeted drugs alter their respective signaling pathways in the brain

To understand the effects of biologically targeted drugs on the developing brain, we studied two separate developmental stages in mice, designated as Paradigm #1 and Paradigm #2 (Fig. 1A–C): Paradigm #1 represents early brain development (ED) and Paradigm #2 represents later brain development (LD; refs. 2, 37). In Paradigm #1, mice received daily injections of drug or vehicle from postnatal day (P)12 until P17 (Fig. 1A and B). During this period, there is a larger population of progenitor and immature cells in the subcortical white matter and hippocampus. In Paradigm #2, mice received daily drug or vehicle from P17 until P22 (Fig. 1A and C). At this age fewer progenitor cells are present as maturation progresses. The daily administration of therapeutics is analogous to repeated dosages necessary in cancer therapy (Fig. 1B and C). We first confirmed developmental expression for these respective drug targets and that the expression of these activated targets decreases with age (Supplementary Fig. S1A). We confirmed that these drugs cross the blood–brain barrier and inhibit their respective targets in the white matter and the hippocampus, and were not lethal (Supplementary Fig. S1B).

### Molecularly targeted agents affect white matter development and function

To determine whether molecularly targeted drugs alter oligodendrocyte development, we studied their effects on different stages of oligodendroglial lineage progression using the cellular markers, Olig2, CC1, and NG2 (Fig. 2A–H).

In Paradigm #1, we observed a significant decrease in the total number of white matter oligodendroglia ($Olig2^+$ cells), mature oligodendrocytes ($CC1^+Olig2^+$ cells), and OPCs ($NG2^+$ cells) after treatment (P18) with all three drugs (Fig. 2C, E, and G). At P30, there continued to be a significant decrease in the total number of oligodendrocytes and mature oligodendrocytes, with recovery noted by adulthood (P60; Fig. 2C and E). The decrease in OPCs at P30 was maintained, but did not reach significance (Fig. 2G). Paradigm #2 did not produce significant changes in the number of total and mature oligodendrocytes by P23 (Fig. 2D and F). However, all three agents did significantly decrease the number of OPCs compared with vehicle (Fig. 2H). While no immediate effect was evident on total and mature oligodendrocyte numbers after treatment, their numbers were significantly decreased at P30 (Fig. 2D and F). Representative IHC examples are presented in Supplementary Fig. S2. Together, these data suggest that decreasing OPCs during development has important consequences on mature oligodendrocyte numbers at a later time point.

To determine effects on myelin protein (MBP) expression, Western blot analysis was conducted on microdissected white matter tissue. In Paradigm #1, MBP was decreased in all drug treatment groups at P18, when compared with vehicle (Supplementary Fig. S3A–S3C). In contrast, in Paradigm #2, no change in MBP expression was detected between drugs and vehicle at P23 and P30 (Supplementary Fig. S3D–S3F).

To define the effects of these drugs on oligodendrocyte development, we analyzed cell proliferation, cell death, and oligodendrogenesis. In both Paradigm #1 and #2, significant decreases in total cell proliferation ($Ki67^+$) and oligodendrocyte proliferation ($Ki67^+Olig2^+$) were found only immediately after treatment (Fig. 3A–D). No difference in proliferation was evident by P30, indicating recovery. The absence of change in total cleaved caspase-3 positive ($Casp\text{-}3^+$) cells and $Casp\text{-}3^+Olig2^+$ cells in the white matter (Fig. 3E–H) in both paradigms indicated no change in cell survival. Because of the significant decreases in oligodendrocyte proliferation immediately after treatment, we evaluated whether the drugs also affected the generation of new oligodendrocytes by utilizing a BrdUrd pulse chase-labeling paradigm that overlaps with drug treatment (Fig. 3I–N). IHC analysis of $BrdUrd^+Olig2^+$ and $BrdUrd^+$ $CC1^+$ at P30 showed that, in both Paradigms, all molecularly targeted drugs significantly decreased the generation and maturation of new oligodendrocytes (Fig. 3J–N; Supplementary Fig. S4A–S4E). Interestingly, in both paradigms, no difference in was observed when BrdUrd pulse labeling was performed post drug exposure (Supplementary Fig. S5A–S5D).

While we have demonstrated that these agents affect white matter oligodendrocytes, we also found that, in both paradigms, astrocyte cells were unaffected [glial fibrillary acidic protein $(GFAP)^+$ glutamine synthetase $(GS)^+$; Supplementary Fig. S6A–S6D] showed and found no differences in GFAP protein expression in both paradigms (Supplementary Fig. S6E–S6H). Therefore, in the white matter, these drugs specifically target oligodendrocytes.

Treatment with these drugs during early development (Paradigm #1) produces significant acute and short-term effects on white matter oligodendrocytes and MBP expression. Although treatment at a later age also affects oligodendrocyte number, proliferation, and maturation, it does not affect MBP expression. The cytostatic property of these agents at either developmental stage did not cause oligodendrocyte cell apoptosis or affect white matter astrocytes.

### White matter behavioral deficits result from treatment with molecularly targeted agents

We tested whether drug treatments affected function using the inclined beam-walking task (33). As previously reported, the number of foot slips while walking on two different-sized beams (2 cm and 1 cm) is a good test of motor coordination as an indicator of subcortical white matter function (33). In Paradigm #1, all drug-treated mice displayed a significantly greater number of foot slips than controls for both beams at 1 month and 2 months of age (Fig. 4A and B). In Paradigm #2, all drug treatments significantly increased the number of foot slips on both beams at 1 month of age (Fig. 4C). However, at 2 months of age, only gefitinib-treated mice showed a significant increase in the number of foot slips on the 1-cm beam (Fig. 4D).

These results indicate that molecularly targeted therapies administered during an earlier developmental age have short- and long-term consequences on a task mediated by the white matter. Sunitinib and rapamycin produce transient short-term effects when administered at a later developmental age; however, gefitinib produces long-term performance deficits.

### Molecularly targeted agents affect specific populations of cells in the hippocampus

Classic chemotherapeutic agents contribute to deficits in hippocampal-dependent learning and memory, likely arising from their cytotoxic effects on neurogenic niches such as the subgranular zone of the hippocampus, thus altering neurogenesis (19). The effects of these newer drugs on the hippocampus and the subgranular zone are unknown.

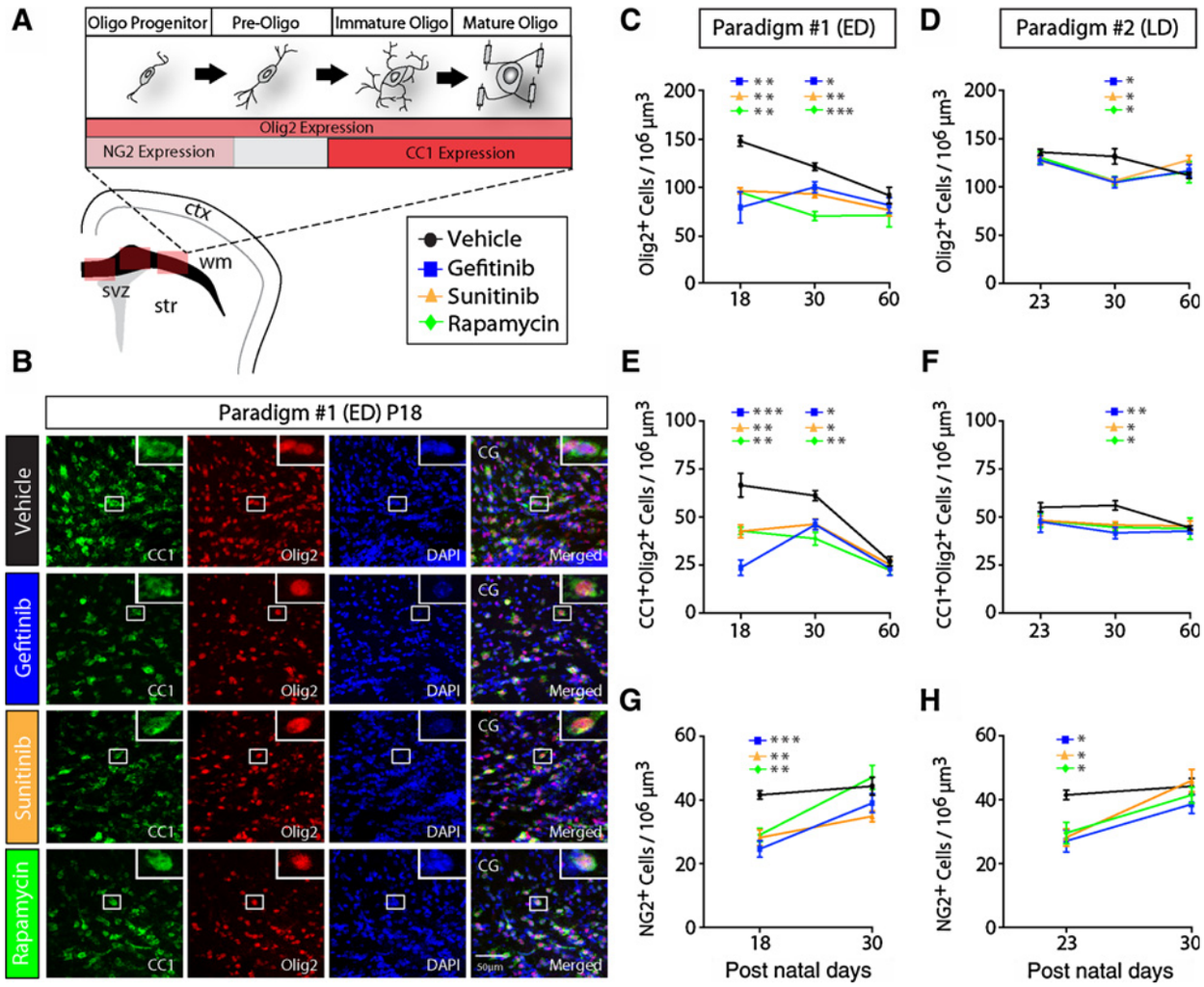


**Figure 2.**

Early treatment with molecularly targeted agents has a greater impact on glial cells in the white matter. **A,** Illustration of the different stages of oligodendrocyte maturation and the subcortical white matter regions used in IHC analysis. **B,** Representative $CC1^+Olig2^+$ confocal IHC images from Paradigm #1 (ED) at P18. **C–H,** Quantification of total ($Olig2^+$ cells; **C** and **D**), mature ($CC1^+Olig2^+$ cells; **E** and **F**), and NG2-expressing oligodendrocytes (**G** and **H**) in the white matter at different time points. $n = 4$–5 mice per all groups and per age; one-way ANOVA, Bonferroni *post hoc* test for individual comparisons. All data are presented as means ± SEM. *, $P < 0.05$; **, $P < 0.01$; ***, $P < 0.005$. Scale bar, 50 μm.

We assessed for changes in hippocampal astrocytes, GFAP protein expression, oligodendrocytes, and neuronal lineage cells in both treatment paradigms (Supplementary Figs. S7A–S7L and S8A–S8D). We found that in both Paradigm #1 and #2 mice, the number of hippocampal astrocytes, as well as GFAP protein levels, was significantly decreased after completing drug treatment (Supplementary Figs. S7A–S7D and S8A–S8D). However, recovery was evident in both Paradigms by P30. When we assessed the total number of oligodendrocytes and mature oligodendrocytes in the hippocampus, no differences were evident in both Paradigms at any age (Supplementary Fig. S7E–S7H), which contrasts with our white matter results (Fig. 2).

To visualize the wide-array of gamma-aminobutyric acid (GABA)-ergic interneurons in the hippocampus, we used *GAD2-IRES-Cre* knock-in mice, mated with a Rosa26-eYFP reporter (38). With all drugs, we found that the number of reporter-positive (RosaYFP) cells in the hippocampus was decreased in Paradigm #1 mice, only immediately after treatment (Supplementary Fig. S7I). At P30, near complete cell recovery was evident except in the mice that received gefitinib. By adulthood (P60), full cellular recovery was evident in all groups. There was no difference in the total number of postmitotic $NeuN^+$ cells (Supplementary Fig. S7J). In Paradigm #2, only gefitinib significantly decreased $RosaYFP^+$ Gad2 lineage cells (Supplementary Fig. S7K). No difference was found in the total number of postmitotic $NeuN^+$ cells (Supplementary Fig. S7L).

It is known that classic chemotherapeutic drugs affect neurogenesis, which may contribute to the cognitive dysfunction (39, 40). In the dentate gyrus, we found that in both Paradigm #1 (ED) and #2 (LD) mice, there was a significant decrease in the number of proliferative cells ($Ki67^+$) immediately after treatment (Fig. 5A and B), but no difference at P30. The number of doublecortin

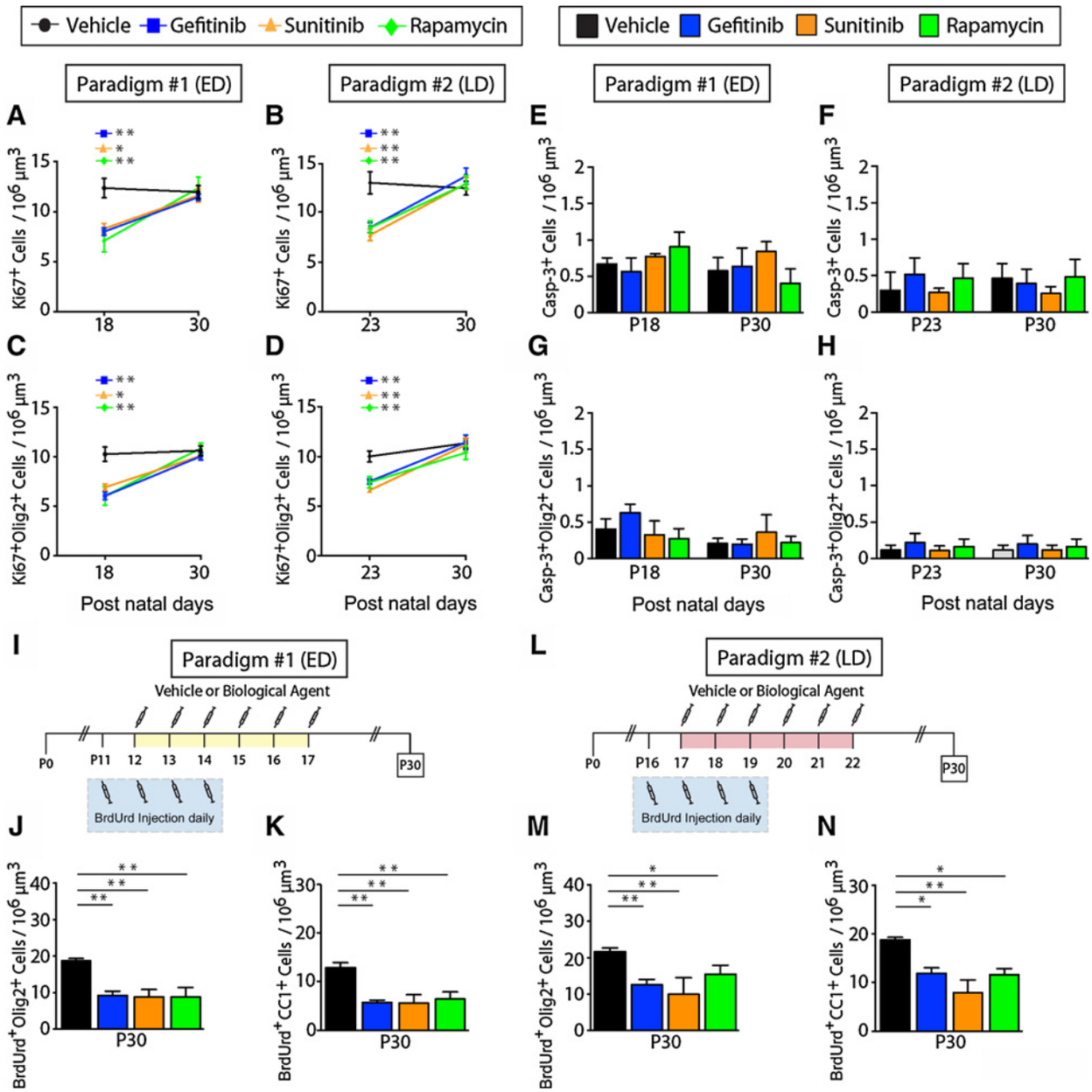


**Figure 3.**

Molecularly targeted agents decrease oligodendrocyte proliferation and newly generated oligodendrocyte number in the white matter. **A–D,** Quantification of total number of proliferating cells ($Ki67^+$; **A** and **B**) and oligodendrocyte proliferation ($Ki67^+Olig2^+$; **C** and **D**) cells for Paradigms #1 and #2. **E–H,** Quantification of total apoptotic ($Casp\text{-}3^+$; **E** and **F**) and oligodendrocyte apoptotic ($Casp\text{-}3^+Olig2^+$; **G** and **H**) cells for Paradigms #1 and #2. **I,** BrdUrd pulse protocol for mice randomized to Paradigm #1. **J** and **K,** Quantification of newly generated oligodendrocyte lineage cells ($BrdUrd^+Olig2^+$) and newly generated mature oligodendrocytes ($BrdUrd^+CC1^+Olig2^+$) in Paradigm #1 at P30. **L,** BrdUrd pulse protocol for mice randomized to Paradigm #2. **M** and **N,** Quantification of newly generated oligodendrocyte lineage cells ($BrdUrd^+Olig2^+$) and newly generated mature oligodendrocytes ($BrdUrd^+CC1^+Olig2^+$) in Paradigm #2 at P30. $n = 4$–5 mice per all groups and per age; one-way ANOVA, Bonferroni *post hoc* test for individual comparisons. All data are presented as means ± SEM. *, $P < 0.05$; **, $P < 0.01$; ***, $P < 0.005$.

positive ($DCx^+$) migratory neuroblasts in a proliferative state ($Ki67^+DCx^+$) was also significantly decreased with all drugs in both Paradigms (Fig. 5C and D). In Paradigm #1 mice, the number of migratory neuroblasts recovered by P30 in animals that received sunitinib and rapamycin but remained significantly decreased in gefitinib-treated mice. In Paradigm #2 mice, the number of migratory neuroblasts cells at P30 was not significantly different.

We also assessed the effects of these drugs on the neural stem cell population in the subgranular zone that expresses Sox2, a

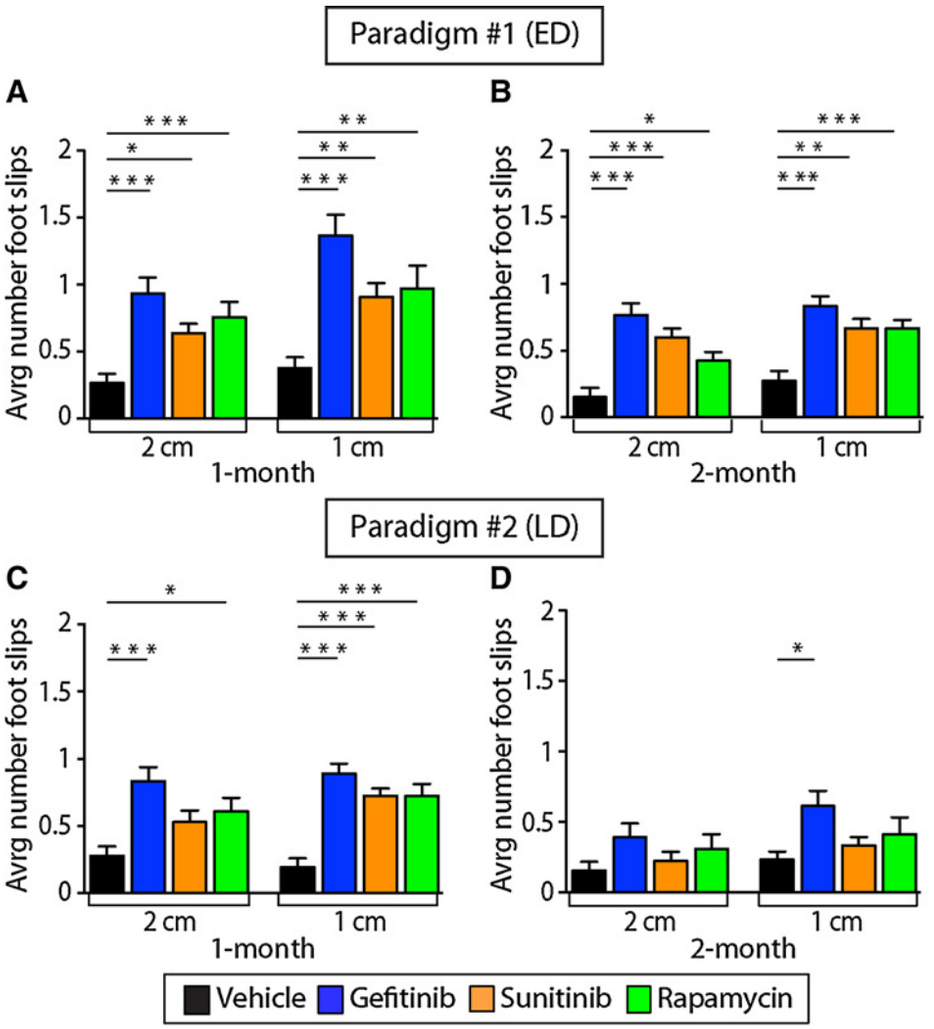


**Figure 4.**
Early treatment with molecularly targeted agents has long-term effects on white matter–dependent behavior. The inclined beam-walking task utilized two different beam widths (2 cm and 1 cm) to assess white matter behavioral performance at 1 month and 2 months of age. **A** and **B,** The number of foot slips in each experimental group in Paradigm #1. **C** and **D,** The number of foot slips in Paradigm #2. $n = 10$–15 mice per all groups and per age; one-way ANOVA, Bonferroni *post hoc* test for individual comparisons. All data are presented as means ± SEM. *, $P < 0.05$; **, $P < 0.01$; ***, $P < 0.005$.

crucial proneurogenic transcription factor in the hippocampus (41). In both Paradigms, all drugs decreased the number of $Sox2^+$-expressing cells (Fig. 5E and F) immediately after completing drug therapy, but there was no change at later time point (P30).

To evaluate the effects on glial precursors in the dentate gyrus, we counted the number of $NG2^+$ progenitor cells in this region. In Paradigm #1, all targeted therapies decreased the number of these cells immediately after treatment, but recovery was evident by P30. In Paradigm #2, only gefitinib reduced the number of NG2-expressing cells at P23 (Fig. 5G and H).

To determine whether neurogenesis still occurs during treatment, we used the BrdUrd pulse chase labeling protocol (see Fig. 3I and L). Colabeling with BrdUrd and NeuN was significantly decreased in both Paradigms and with all drugs, compared with vehicle treatment (Fig. 5I and J). Similar to the white matter, $Casp\text{-}3^+$ cells in the hippocampus was not altered in both Paradigms (Fig. 5K and L).

Together, our results demonstrate that molecularly targeted drugs have significant cellular effects with respect to hippocampal astrocyte numbers, GFAP expression, and GAD2-lineage cells.

### Molecularly targeted agents impair nonspatial and spatial memory

We tested whether treatment with these targeted therapies at different developmental stages have long-term effects on hippocampal-dependent nonspatial and spatial memory. Recognition memory, a type of nonspatial memory, is commonly assessed in rodents with the use of the novel object recognition test (42, 43). The novel object recognition test was performed in naïve mice for both experimental Paradigms at 1 month and 2 months of age. In both paradigms, all treated mice exhibited a significant decrease in the percentage of time spent with the novel object at 1 month of age (Fig. 6A and B). At 2 months, only gefitinib- and rapamycin-treated mice continued to exhibit significant deficits, whereas the sunitinib group had only marginal ($P = 0.06$) memory impairment (Fig. 6A). In Paradigm #2 mice, only those that received gefitinib had significant deficits evident in adulthood (2 months of age; Fig. 6B).

The second behavioral test used to test hippocampal-dependent spatial memory was the Y-maze (44). In both Paradigms, all mice treated with molecularly targeted agents demonstrated a significant decrease in the percentage of unique alternations

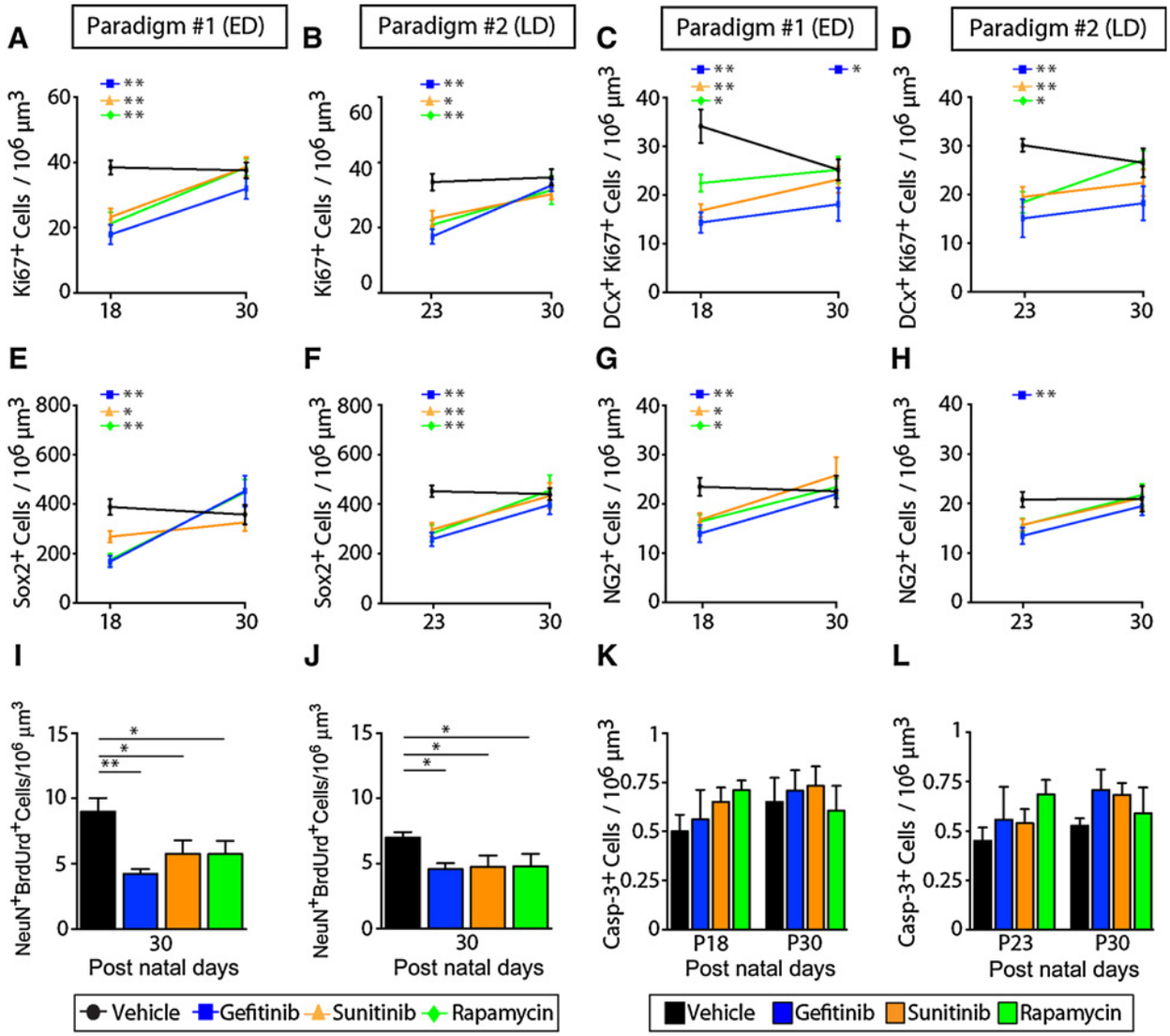


**Figure 5.**

Molecularly targeted agents inhibit cell proliferation and neurogenesis in the hippocampus. **A** and **B,** Proliferation ($Ki67^+$) was quantified in the hippocampal dentate gyrus in Paradigms #1 and #2. **C** and **D,** The number of immature neuronal-lineage cells in a proliferative state ($DCx^+Ki67^+$) was quantified for both Paradigms. **E–H,** Other immature cell populations, such as Sox2 (**E** and **F**) and NG2 (**G** and **H**) were also quantified. **I** and **J,** Using the BrdUrd pulse protocol for Paradigms #1 and #2 outlined in Fig. 3I and L, respectively, we quantified the total number of $BrdUrd^+$ cells that differentiated to $NeuN^+$ in the hippocampus. **K** and **L,** In both paradigms, apoptotic cell death was quantified for each of the experimental groups using Casp-3 immunostaining. $n = 4$–5 mice per all groups and per age; one-way ANOVA, Bonferroni *post hoc* test for individual comparisons. All data are presented as means ± SEM. *, $P < 0.05$; **, $P < 0.01$; ***, $P < 0.005$.

at 1 month of age (Fig. 6C and D). Another assessment of hippocampal-dependent spatial memory is the Barnes maze (45). This test was performed only at 2 months of age because of the difficulty training younger mice. After a 5-day training period, the mice were tested for short-term (24 hours after the last day of training, Probe Day 1) and long-term (5 days later, Probe Day 5) memory. Paradigm #1 produced a significant increase in the number of primary errors in all three drug treatment groups at Probe Days 1 and 5 (Fig. 6E). In Paradigm #2, only gefitinib-treated mice demonstrated a significant increase in the number of primary errors at 2 months of age for both probe trial days (Fig. 6F).

Together, these results demonstrate that treatment at an early age has more significant short- and long-term consequences on learning and memory than treatment at a later age. While later treatment produces effects shortly after treatment, these effects do not persist in the long-term after sunitinib and rapamycin. However, treatment with gefitinib at both earlier and later developmental stages exhibits detrimental effects on long-term cognitive function.

### Single-dose treatment affects progenitor cells

Our results indicate that these drugs administered over several days have a significant effect on progenitor cells and generation of

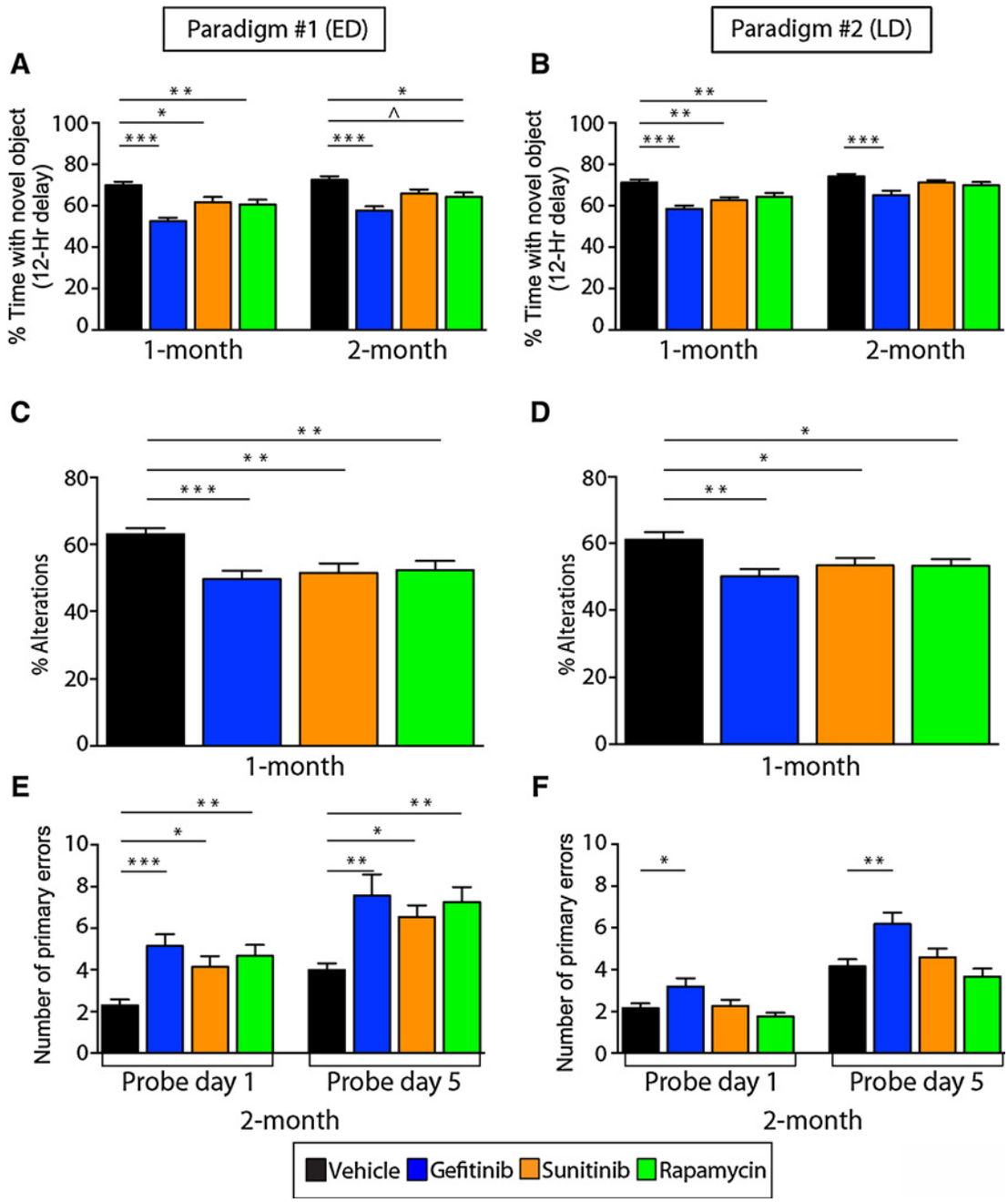


**Figure 6.**

Early treatment with molecularly targeted agents has long-term effects on hippocampal-dependent memory. **A** and **B,** Recognition memory was tested at 1 month and 2 months of age in both paradigms using the novel object recognition test. The recognition index was assessed after a 12-hour delay between the sample and test phase. **C** and **D,** Spatial memory was tested using the spontaneous alternation behavior memory test, where the percent alternation was calculated in all experimental groups at 1 month of age in Paradigm #1 and #2. **E** and **F,** The Barnes maze assessed spatial memory at 2 months of age. The histograms present the number of primary errors on probe day 1 (short-term memory) and probe day 5 (long-term memory). $n = 10$–15 mice per all groups and per age; one-way ANOVA, Bonferroni *post hoc* test for individual comparisons. All data are presented as means ± SEM. ^, $P = 0.06$; *, $P < 0.05$; **, $P < 0.01$; ***, $P < 0.005$.

new oligodendrocytes and neurons. While most cancer therapy requires repeated administration of therapy over time, we tested whether a single dose of drug administered at P12 (ED) or P17 (LD) has short and long-term cellular and behavioral deficits (refer to Supplementary Fig. S9A–S9P). Tissue was collected 24 hours after single dose treatment and at P30. At both developmental stages (ED and LD), a single dose decreased the number of white matter OPCs ($NG2^+$), but not mature oligodendrocytes

($CC1^+Olig2^+$) after treatment (Supplementary Fig. S9B, S9C, S9J, and S9K). No effect was evident at P30 or on subcortical white matter behavior at 1 month of age (Supplementary Fig. S9D and S9L). In the hippocampus, a single dose of drug administered at either developmental stage resulted in a significant decrease in $Sox2^+$ progenitor cells (Supplementary Fig. S9E and S9M) and proliferating neuroblasts ($DCx^+Ki67^+$; Supplementary Fig. S9F and S9N). Both populations of cells recovered by P30. No effect was evident on postmitotic neuronal cells and on hippocampal-dependent recognition memory (Supplementary Fig. S9G, S9H, S9O, and S9P). These data support our finding that a single dose of these cytostatic molecularly targeted drugs transiently decreases progenitor cells. This contrasts with the short and long-term consequences of repeated doses.

**Treatment with targeted therapies has no effect in adult mice**

To determine whether the effects we observed are age-specific, we administered the molecularly targeted drugs in adult mice (Supplementary Fig. S10A). In contrast with younger-treated mice, the total number of white matter oligodendrocytes, mature oligodendrocytes, or OPCs remained unchanged (Supplementary Fig. S10B–S10D). During the inclined beam-walking task 1 week after treatment, no difference in the number of foot slips was evident (Supplementary Fig. S10E). In the hippocampus, the number of Gad2Cre-lineage reporter cells and the total number of NeuN-positive postmitotic cells was not significantly different from controls (Supplementary Fig. S10F and S10G). Furthermore, treatment in adults failed to produce differences in novel object recognition test (Supplementary Fig. S10H).

These results demonstrate that, unlike treatment at younger ages, treatment in adulthood produces no cellular effects in the white matter or hippocampus and does not alter behavioral function associated with these brain regions.

**Environmental enrichment improves behavioral deficits**

The use of cognitive, social stimulation, and physical therapies are becoming increasingly important for the treatment of disease and treatment-associated morbidities (46). In rodents, environmental enrichment is used to stimulate the brain by social, novel, and complex surroundings with the ability for increased physical activity. Recent rodent studies have demonstrated that environmental enrichment is effective in improving both sensorimotor and hippocampal behavioral performance through enhanced neurogenesis (36, 47–49).

To assess whether environmental enrichment would improve abnormalities from molecularly targeted anticancer treatment, we selected the group with the most severe deficits: mice treated at a younger age. Paradigm #1 mice were subjected to 8 to 12 hours of daily environmental enrichment from P17 to P30 following drug administration (Fig. 7A). We then analyzed the white matter and hippocampus by IHC, and compared the results with those of nonenriched controls. Enrichment prevented the maturation deficits of oligodendrocytes ($BrdUrd^+CC1^+$; Fig. 7B) and neurons ($BrdUrd^+NeuN^+$; Fig. 7C).

The inclined beam-walking task showed that drug-treated mice that received enrichment performed significantly better than drug-treated mice in the control environment (Fig. 7D; ref. 33). Similarly, enrichment also improved recognition memory, compared with the nonenriched control group (Fig. 7E).

These results thereby indicate that environmental enrichment is an effective intervention to improve white matter- and hippocampal-dependent behavioral performance following administration of molecularly targeted anticancer agents.

## Discussion

Our study is the first to demonstrate that the developing brain's white matter and hippocampus are most vulnerable to molecularly targeted drugs administered at an early age. While administration of these drugs at a later developmental stage (from P17 to P22) did produce negative effects, they were not as pronounced. Interestingly, treatment with these drugs in the mature brain did not produce cellular or behavioral deficits. While the younger developing brain is most vulnerable to these molecularly targeted agents, reversal was possible by promoting brain plasticity through increased social interaction and physical activity (i.e., environmental enrichment). This indicates that promoting brain plasticity with timely intervention improves the age-dependent side effects of molecularly targeted drug therapy.

Brain development is a continuum that begins during early gestation and continues until young adulthood, with the most rapid growth and maturation of progenitor cells occurring during the first several years of life (37). At the cellular level, these events are dependent on a coordinated balance between expression and activation of different growth factors (EGF, VEGF, and PDGF), their respective receptors, and the multiple intracellular signaling pathways associated with these receptors. One of the major intracellular pathways activated by growth factor receptors is PI3K/protein kinase B (AKT)/mTOR. This pathway is crucial for proliferation, growth, angiogenesis, and survival. Upon completion of development and with increasing age, growth factors and their respective receptors take on different roles, such as cell maintenance, or participate in the endogenous recovery after injury. However, if the receptors or their intracellular signaling pathways become dysfunctional, tumorigenesis may ensue.

Two critical brain structures that continue to mature in early childhood and adolescence are the subcortical white matter and the hippocampus. These structures are important for sensorimotor and cognitive function and are affected in patients undergoing treatment for cancer (40, 41). The neurotoxic effects in pediatric and adult cancer treatments are associated with both localized therapy, such as radiation, and systemic chemotherapeutic agents (41, 50, 51). However, infants and children are more susceptible to neurologic and neurosensory sequelae than adults. These conventional treatments are associated with white matter abnormalities on diffusion tensor imaging, as well as posttreatment executive and cognitive dysfunction. At the cellular level, conventional chemotherapeutics exert toxic effects on neural progenitor cells in neurogenic niches and oligodendrocytes in the adult brain (52, 53). Molecularly targeted therapeutics that specifically target dysregulated pathways are promising treatments for these cancers.

In the current study, we found that in the subcortical white matter of mice treated at a young age, the total number of oligodendrocytes and mature oligodendrocytes was significantly decreased immediately after treatment and remained low even into young adulthood. This was not observed in mice that began treatment at a later age. The number of immature NG2-expressing OPCs decreased, followed by a decrease several days later in the number of mature oligodendrocytes. No effects were evident in adulthood, probably because there are fewer numbers of progenitor cells in the adult brain.

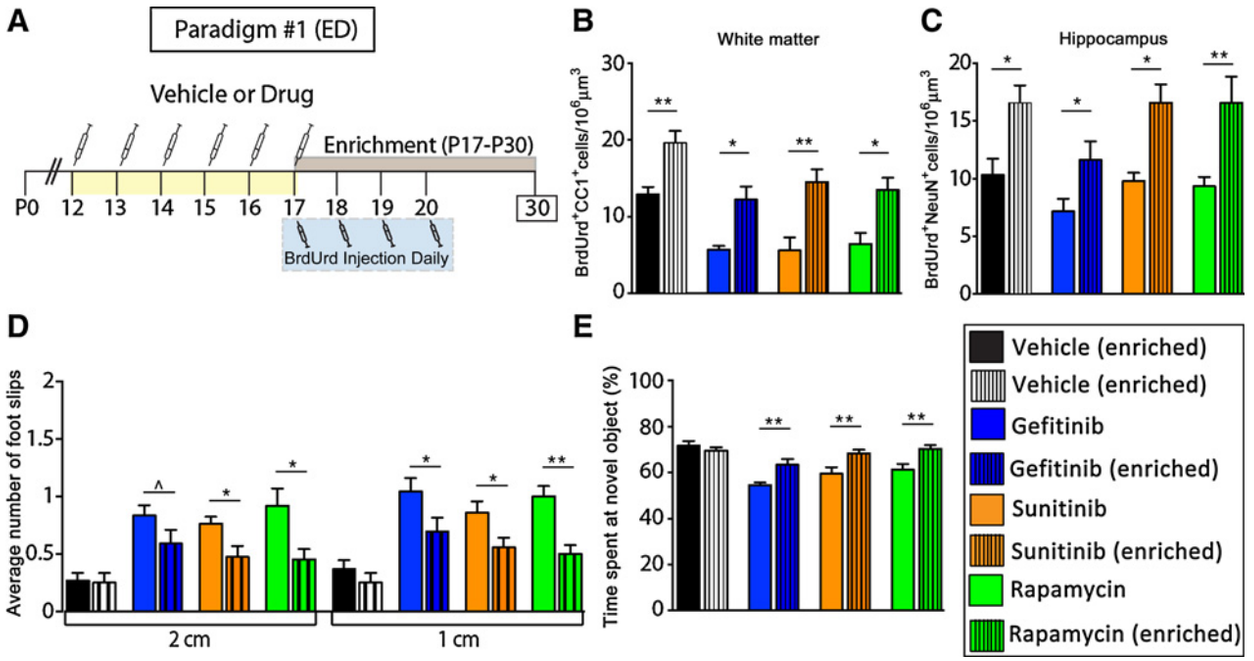


**Figure 7.**

Environmental enrichment reverses behavioral deficits. **A,** Experimental protocol of vehicle or drug administration, followed by randomization to either receive 12 hours a day of environmental enrichment from P17–P30 or remain in typical housing environment. BrdUrd was administered daily from P17–P20. Behavioral testing was performed between P30 and P32. **B,** Quantification of newly generated mature oligodendrocytes ($BrdUrd^+CC1^+Olig2^+$) at P30. **C,** Quantification of newly generated postmitotic neurons (BrdUrd+NeuN+) at P30. **D,** The average number of foot slips on the 2 cm and 1 cm inclined beam-walking task. **E,** Recognition memory was tested using the novel object recognition memory paradigm with a 12-hour delay between sample and test phase. In the test phase, the percent time spent with the novel object was calculated. For **B** and **C**, $n = 4$ mice per all groups. For **D** and **E**, $n = 10$–15 mice per all groups and per age. A one-way ANOVA, followed by unpaired $t$ test comparing nonenriched with enrichment. All data are presented as means ± SEM. ^, $P = 0.05$; *, $P < 0.05$; **, $P < 0.01$; ***, $P < 0.005$.

Although the molecularly targeted agents significantly decreased white matter proliferation and oligodendrogenesis at both treatment ages, they did not affect apoptosis. Assessment of behavioral outcomes using a white matter-specific behavioral task showed that mice in the younger treatment group had significant short- and long-term sensorimotor deficits, while the older treated group deficits were only evident at P30 (young adulthood) but did not persist. Interestingly, mice treated as adults with all molecularly targeted agents exhibited no sensorimotor behavioral deficits.

The phosphorylated molecular targets of these drugs are most abundant between P12 and P17 (Supplementary Fig. S1A). However, with increasing age, these pathways are less active (Supplementary Fig. S1A). The LD paradigm, where treatment ends at P22, an age when targets have clearly declined, produces smaller cellular changes at P23. Indeed, using the datasets presented in Fig. 2, $t$ test analysis of the extent of change in cell densities relative to vehicle revealed that, immediately after treatment, ED reduces $Olig2^+$ ($P < 0.01$) and CC1+$Olig2^+$ ($P < 0.05$) cells significantly more than LD, irrespective of drug. These differences may form a cellular basis underlying the greater persistence of behavioral deficit arising in the ED treatment group. As molecular targets are no longer phosphorylated at high levels in adulthood (Supplementary Fig. S1A), adult treatment produces neither cellular change nor behavioral deficit. Interestingly, quantitative differences between ED and LD could not be found among the cellular markers we had analyzed in the hippocampus, suggesting that other factors (e.g., other neuronal cells, myelin ultrastructure, changes to circuitry) may contribute to persistence of hippocampal-dependent deficits preferentially induced in the early treatment (ED) paradigm.

Unlike the white matter, astrocytes of the hippocampus in both early and later treatment groups were significantly decreased immediately after the completion of treatment. However, the drugs did not affect hippocampal oligodendrocytes. GAD2-expressing cells in the hippocampus were affected by these drugs in the early-treated mice and by gefitinib only in the later-treated mice. Similar to the white matter, the molecularly targeted drugs decreased proliferation, progenitor cells, and hippocampal neurogenesis in both age groups. These drugs also did not significantly change apoptotic cell death, supporting a mechanism of cytostasis, rather than cellular toxicity. Indeed, the short-lived nature of drug activity is further demonstrated in two single-dose experiments (Supplementary Fig. S9). This property, combined with the innate regenerative response following injury, promotes the observed cell replacement and recovery in both WM and hippocampus at P30. The normal developmental decline in proliferating progenitor cell populations with age also adds to the perceived recovery of cell proliferation after drug treatment.

Patients undergoing cancer treatment have immediate and long-term difficulties with cognitive performance, such as learning and memory. However, it is difficult to discern whether these are the result of treatment or of both cancer and treatment. This study evaluated whether treatment alone affects hippocampal

function. Recognition and spatial memory were impaired in younger-treated mice. While mice treated at a later age did have impairement early on, these deficits persisted into adulthood only in the gefitinib-treated mice. No effect was evident in any drug group in those treated in adulthood, indicating that the behavioral effects of these drugs are developmentally restricted and do not manifest in the adult treatment groups.

The short- and long-term negative effects of these drugs on the developing brain treated at an earlier age raise the important question whether these deficits are amendable to reversal. Cognitive and physical therapy are being investigated as a potential nonpharmacologic approach to improve cognition and quality of life after cancer treatment in both pediatric and adult patients. To mimic these therapies in rodents, we used an environmental enrichment paradigm in which mice are housed for a short period of time each day in a larger, socially enriched cage containing novel stimuli and a running wheel to increase physical activity. The enrichment was initiated after completing drug therapy to mimic the usual clinical scenario in cancer patients. The improvement in both white matter oligodendrogenesis and hippocampal neurogenesis, we observed in mice subjected to enrichment was consistent with the fewer deficits observed with enrichment. The potential reversal of deficits with a regimen of increased social, physical, and cognitive activity thus reinforces the important role of such regimes in improving morbidity (47, 51).

A limitation of our study is that treatment with the three commercially available, molecularly targeted therapeutic drugs was performed in healthy mice without cancer and each animal received only a single agent. However, we wanted to test whether these drugs alone affected the brain. We know from preclinical studies of these individual agents that they target cancer cells and decrease cancer cell growth *in vitro* and *in vivo*. However, those studies were performed in adults and did not assess unaffected brain regions. In clinical practice, these drugs are used in conjunction with conventional therapies, which often complicates our understanding of the cellular and behavioral effects from these agents.

In summary, our results demonstrate that the early developing brain is selectively vulnerable to molecularly targeted drugs used for cancer therapy. This class of drugs affects cellular development, proliferation, and maturation when administered at a young age. The result is impairment of white matter and hippocampal function. Importantly, these effects can be attenuated by exposure to a stimulating cognitive and physical environment. These findings have broad clinical implications for the pediatric population, as the therapies are not only being used for cancers, but also for other medical conditions. For example, intravitreal injection of molecularly targeted VEGF inhibitors is currently being used in preterm infants with retinopathy of prematurity (54). Despite intravitreal administration, high plasma levels of the drug and decreased serum levels of VEGF occur (55). This suggests that that brain toxicity may be an important issue as these drugs can cross the blood–brain barrier.

Further research regarding the impact of molecularly targeted drugs and the possible additive effects of traditional cancer treatments on the developing brain is necessary. Our results are not meant to discourage physicians from using these targeted therapies in young patients, but to foster an awareness of their effects on the developing brain. Further studies on the neurodevelopmental and cognitive effects of molecularly targeted drugs administered to pediatric populations are necessary to minimize morbidity.

## Disclosure of Potential Conflicts of Interest

No potential conflicts of interest were disclosed.

## Disclaimer

The contents of this article are solely the responsibility of the authors and do not represent the official views of the DC-IDDRC or the NIH.

## Authors' Contributions

**Conception and design:** J. Scafidi, V. Gallo
**Development of methodology:** J. Scafidi, J. Ritter, V. Gallo
**Acquisition of data (provided animals, acquired and managed patients, provided facilities, etc.):** J. Scafidi, J. Ritter, B.M. Talbot, J. Edwards
**Analysis and interpretation of data (e.g., statistical analysis, biostatistics, computational analysis):** J. Scafidi, J. Ritter, V. Gallo
**Writing, review, and/or revision of the manuscript:** J. Scafidi, J. Ritter, B.M. Talbot, L.-J. Chew, V. Gallo
**Administrative, technical, or material support (i.e., reporting or organizing data, constructing databases):** J. Scafidi, J. Ritter, B.M. Talbot, J. Edwards
**Study supervision:** J. Scafidi, V. Gallo

## Acknowledgments

This work was supported by the National Brain Tumor Society (to J. Scafidi), The Children Brain Tumor Foundation (to J. Scafidi), NIH grants K08NS073793 (to J. Scafidi), R01NS099461 (to J. Scafidi), and 1U54HD090257 (to V. Gallo).

Microscopic analysis was carried out at the Children's Research Institute (CRI) Light Microscopy and Image Analysis Core supported by CRI and NIH1U54HD090257. This project was supported in part by the District of Columbia Intellectual and Developmental Disabilities Research Center Award (DC-IDDRC).

The costs of publication of this article were defrayed in part by the payment of page charges. This article must therefore be hereby marked *advertisement* in accordance with 18 U.S.C. Section 1734 solely to indicate this fact.

Received July 27, 2017; revised January 12, 2018; accepted February 9, 2018; published first March 20, 2018.

## References

1. Ostrom QT, Gittleman H, Fulop J, Liu M, Blanda R, Kromer C, et al. CBTRUS statistical report: primary brain and central nervous system tumors diagnosed in the United States in 2008–2012. Neuro Oncol 2015;17Suppl 4:iv1–iv62.
2. Gittleman HR, Ostrom QT, Rouse CD, Dowling JA, de Blank PM, Kruchko CA, et al. Trends in central nervous system tumor incidence relative to other common cancers in adults, adolescents, and children in the United States, 2000 to 2010. Cancer 2015;121:102–12.
3. Armstrong GT, Liu Q, Yasui Y, Huang S, Ness KK, Leisenring W, et al. Long-term outcomes among adult survivors of childhood central nervous system malignancies in the Childhood Cancer Survivor Study. J Natl Cancer Inst 2009;101:946–58.
4. Witsch E, Sela M, Yarden Y. Roles for growth factors in cancer progression. Physiology (Bethesda) 2010;25:85–101.
5. Nageswara Rao AA, Packer RJ. Impact of molecular biology studies on the understanding of brain tumors in childhood. Curr Oncol Rep 2012;14:206–12.
6. Keppler-Noreuil KM, Parker VE, Darling TN, Martinez-Agosto JA. Somatic overgrowth disorders of the PI3K/AKT/mTOR pathway & therapeutic strategies. Am J Med Genet C Semin Med Genet 2016;172:402–21.

7. Miller JJ, Wen PY. Emerging targeted therapies for glioma. Expert Opin Emerg Drugs 2016;21:441–52.
8. Takei N, Nawa H. mTOR signaling and its roles in normal and abnormal brain development. Front Mol Neurosci 2014;7:28.
9. Rogers HA, Estranero J, Gudka K, Grundy RG. The therapeutic potential of targeting the PI3K pathway in pediatric brain tumors. Oncotarget 2017; 8:2083–95.
10. Nageswara Rao AA, Scafidi J, Wells EM, Packer RJ. Biologically targeted therapeutics in pediatric brain tumors. Pediatr Neurol 2012;46: 203–11.
11. Pollack IF, Stewart CF, Kocak M, Poussaint TY, Broniscer A, Banerjee A, et al. A phase II study of gefitinib and irradiation in children with newly diagnosed brainstem gliomas: a report from the Pediatric Brain Tumor Consortium. Neuro Oncol 2011;13:290–7.
12. Wetmore C, Daryani VM, Billups CA, Boyett JM, Leary S, Tanos R, et al. Phase II evaluation of sunitinib in the treatment of recurrent or refractory high-grade glioma or ependymoma in children: a children's Oncology Group Study ACNS1021. Cancer Med 2016;5:1416–24.
13. Wolff JE, Brown RE, Buryanek J, Pfister S, Vats TS, Rytting ME. Preliminary experience with personalized and targeted therapy for pediatric brain tumors. Pediatr Blood Cancer 2012;59:27–33.
14. Habib SL, Al-Obaidi NY, Nowacki M, Pietkun K, Zegarska B, Kloskowski T, et al. Is mTOR inhibitor good enough for treatment all tumors in TSC patients? J Cancer 2016;7:1621–31.
15. Sasongko TH, Ismail NF, Nik Abdul Malik NM, Zabidi-Hussin ZA. Rapamycin and its analogues (rapalogs) for Tuberous Sclerosis Complex-associated tumors: a systematic review on non-randomized studies using meta-analysis. Orphanet J Rare Dis 2015;10:95.
16. Thaker NG, Pollack IF. Molecularly targeted therapies for malignant glioma: rationale for combinatorial strategies. Expert Rev Neurother 2009; 9:1815–36.
17. Wells EM, Nageswara Rao AA, Scafidi J, Packer RJ. Neurotoxicity of biologically targeted agents in pediatric cancer trials. Pediatr Neurol 2012; 46:212–21.
18. Packer RJ, Pfister S, Bouffet E, Avery R, Bandopadhayay P, Bornhorst M, et al. Pediatric low-grade gliomas: implications of the biologic era. Neuro Oncol 2017;19:750–61.
19. Gibson E, Monje M. Effect of cancer therapy on neural stem cells: implications for cognitive function. Curr Opin Oncol 2012;24:672–8.
20. Uda S, Matsui M, Tanaka C, Uematsu A, Miura K, Kawana I, et al. Normal development of human brain white matter from infancy to early adulthood: a diffusion tensor imaging study. Dev Neurosci 2015; 37:182–94.
21. Huang H, Shu N, Mishra V, Jeon T, Chalak L, Wang ZJ, et al. Development of human brain structural networks through infancy and childhood. Cereb Cortex 2015;25:1389–404.
22. Uematsu A, Matsui M, Tanaka C, Takahashi T, Noguchi K, Suzuki M, et al. Developmental trajectories of amygdala and hippocampus from infancy to early adulthood in healthy individuals. PLoS One 2012;7: e46970.
23. Matsuzawa J, Matsui M, Konishi T, Noguchi K, Gur RC, Bilker W, et al. Age-related volumetric changes of brain gray and white matter in healthy infants and children. Cereb Cortex 2001;11:335–42.
24. Tanaka C, Matsui M, Uematsu A, Noguchi K, Miyawaki T. Developmental trajectories of the fronto-temporal lobes from infancy to early adulthood in healthy individuals. Dev Neurosci 2012;34:477–87.
25. Monje M, Fisher PG. Neurological complications following treatment of children with brain tumors. J Pediatr Rehabil Med 2011;4:31–6.
26. Monje M, Thomason ME, Rigolo L, Wang Y, Waber DP, Sallan SE, et al. Functional and structural differences in the hippocampus associated with memory deficits in adult survivors of acute lymphoblastic leukemia. Pediatr Blood Cancer 2013;60:293–300.
27. Cox LE, Ashford JM, Clark KN, Martin-Elbahesh K, Hardy KK, Merchant TE, et al. Feasibility and acceptability of a remotely administered computerized intervention to address cognitive late effects among childhood cancer survivors. Neurooncol Pract 2015;2:78–87.
28. Butler RW, Copeland DR, Fairclough DL, Mulhern RK, Katz ER, Kazak AE, et al. A multicenter, randomized clinical trial of a cognitive remediation program for childhood survivors of a pediatric malignancy. J Consult Clin Psychol 2008;76:367–78.
29. Heimberger AB, Learn CA, Archer GE, McLendon RE, Chewning TA, Tuck FL, et al. Brain tumors in mice are susceptible to blockade of epidermal growth factor receptor (EGFR) with the oral, specific, EGFR-tyrosine kinase inhibitor ZD1839 (Iressa). Clin Cancer Res 2002;8:3496–502.
30. Mendel DB, Laird AD, Xin X, Louie SG, Christensen JG, Li G, et al. In vivo antitumor activity of SU11248, a novel tyrosine kinase inhibitor targeting vascular endothelial growth factor and platelet-derived growth factor receptors: determination of a pharmacokinetic/pharmacodynamic relationship. Clin Cancer Res 2003;9:327–37.
31. Potapova O, Laird AD, Nannini MA, Barone A, Li G, Moss KG, et al. Contribution of individual targets to the antitumor efficacy of the multitargeted receptor tyrosine kinase inhibitor SU11248. Mol Cancer Ther 2006;5:1280–9.
32. Arcella A, Biagioni F, Antonietta Oliva M, Bucci D, Frati A, Esposito V, et al. Rapamycin inhibits the growth of glioblastoma. Brain Res 2013;1495: 37–51.
33. Scafidi J, Hammond TR, Scafidi S, Ritter J, Jablonska B, Roncal M, et al. Intranasal epidermal growth factor treatment rescues neonatal brain injury. Nature 2014;506:230–4.
34. Clark RE, Zola SM, Squire LR. Impaired recognition memory in rats after damage to the hippocampus. J Neurosci 2000;20:8853–60.
35. Hughes RN. The value of spontaneous alternation behavior (SAB) as a test of retention in pharmacological investigations of memory. Neurosci Biobehav Rev 2004;28:497–505.
36. Chakrabarti L, Scafidi J, Gallo V, Haydar TF. Environmental enrichment rescues postnatal neurogenesis defect in the male and female Ts65Dn mouse model of Down syndrome. Dev Neurosci 2011;33:428–41.
37. Semple BD, Blomgren K, Gimlin K, Ferriero DM, Noble-Haeusslein LJ. Brain development in rodents and humans: Identifying benchmarks of maturation and vulnerability to injury across species. Prog Neurobiol 2013;106–107:1–16.
38. Taniguchi H, He M, Wu P, Kim S, Paik R, Sugino K, et al. A resource of Cre driver lines for genetic targeting of GABAergic neurons in cerebral cortex. Neuron 2011;71:995–1013.
39. Monje M, Dietrich J. Cognitive side effects of cancer therapy demonstrate a functional role for adult neurogenesis. Behav Brain Res 2012;227:376–9.
40. Wefel JS, Schagen SB. Chemotherapy-related cognitive dysfunction. Curr Neurol Neurosci Rep 2012;12:267–75.
41. Suh H, Consiglio A, Ray J, Sawai T, D'Amour KA, Gage FH. In vivo fate analysis reveals the multipotent and self-renewal capacities of Sox2+ neural stem cells in the adult hippocampus. Cell Stem Cell 2007;1:515–28.
42. Cohen SJ, Munchow AH, Rios LM, Zhang G, Asgeirsdottir HN, Stackman RW Jr. The rodent hippocampus is essential for nonspatial object memory. Curr Biol 2013;23:1685–90.
43. Leger M, Quiedeville A, Bouet V, Haelewyn B, Boulouard M, Schumann-Bard P, et al. Object recognition test in mice. Nat Protoc 2013;8:2531–7.
44. Farley SJ, McKay BM, Disterhoft JF, Weiss C. Reevaluating hippocampus-dependent learning in FVB/N mice. Behav Neurosci 2011;125:871–8.
45. Attar A, Liu T, Chan WT, Hayes J, Nejad M, Lei K, et al. A shortened Barnes maze protocol reveals memory deficits at 4-months of age in the triple-transgenic mouse model of Alzheimer's disease. PLoS One 2013; 8:e80355.
46. Kucherer S, Ferguson RJ. Cognitive behavioral therapy for cancer-related cognitive dysfunction. Curr Opin Support Palliat Care 2017;11:46–51.
47. Yang Y, Zhang J, Xiong L, Deng M, Wang J, Xin J, et al. Cognitive improvement induced by environment enrichment in chronic cerebral hypoperfusion rats: a result of upregulated endogenous neuroprotection? J Mol Neurosci 2015;56:278–89.
48. Fan Y, Liu Z, Weinstein PR, Fike JR, Liu J. Environmental enrichment enhances neurogenesis and improves functional outcome after cranial irradiation. Eur J Neurosci 2007;25:38–46.
49. Ohlsson AL, Johansson BB. Environment influences functional outcome of cerebral infarction in rats. Stroke 1995;26:644–9.
50. Ris MD, Walsh K, Wallace D, Armstrong FD, Holmes E, Gajjar A, et al. Intellectual and academic outcome following two chemotherapy regimens and radiotherapy for average-risk medulloblastoma: COG A9961. Pediatr Blood Cancer 2013;60:1350–7.
51. Kahalley LS, Conklin HM, Tyc VL, Hudson MM, Wilson SJ, Wu S, et al. Slower processing speed after treatment for pediatric brain tumor and acute lymphoblastic leukemia. Psychooncology 2013;22:1979–86.

52. Han R, Yang YM, Dietrich J, Luebke A, Mayer-Proschel M, Noble M. Systemic 5-fluorouracil treatment causes a syndrome of delayed myelin destruction in the central nervous system. J Biol 2008; 7:12.
53. Dietrich J, Han R, Yang Y, Mayer-Proschel M, Noble M. CNS progenitor cells and oligodendrocytes are targets of chemotherapeutic agents in vitro and in vivo. J Biol 2006;5:22.
54. Sankar MJ, Sankar J, Mehta M, Bhat V, Srinivasan R. Anti-vascular endothelial growth factor (VEGF) drugs for treatment of retinopathy of prematurity. Cochrane Database Syst Rev 2016;2:CD009734.
55. Wu WC, Lien R, Liao PJ, Wang NK, Chen YP, Chao AN, et al. Serum levels of vascular endothelial growth factor and related factors after intravitreous bevacizumab injection for retinopathy of prematurity. JAMA Ophthalmol 2015;133:391–7.